Probing Microstructure of Acetonitrile−Water Mixtures by Using Two-Dimensional Infrared Correlation Spectroscopy

Eric M. Tee, Aminiel Awichi, and Wei Zhao*

Department of Chemistry, University of Arkansas, 2801 South University Avenue, Little Rock, Arkansas 72204

Received: March 15, 2002; In Final Form: May 6, 2002

Acetonitrile−water mixtures are a unique model system for implementing a new family of coherent two-dimensional (2D) vibrational spectroscopy−doubly vibrationally enhanced (DOVE) four wave mixing (FWM) spectroscopy for structure analysis of hydrogen-bonded systems. These mixtures often have a heterogeneous microstructure that consists of acetonitrile (CH_3CN) or water clusters. There are two types of CH_3CN environments in mixtures-free CH_3CN species and hydrogen-bonded CH_3CN species. To design new DOVE−FWM experiments and interpret DOVE−FWM spectra, it is crucial to have a complete structure information regarding this model system. In this work, we have used a highly sensitive spectroscopic method, 2D infrared (IR) correlation spectroscopy for probing structure information of the mixtures (a 50:50 mol % CH_3CN-H_2O solution, a 50:50 mol % CH_3CN-D_2O solution and a 38:62 mol % CH_3CN-D_2O solution) under temperature perturbation. In addition to two cross-peaks at 2253 and 2259 cm^{-1}, corresponding to the C≡N stretch of free acetonitrile molecules and hydrogen-bonded acetonitrile molecules, respectively, the 2D correlation spectra show a new feature at 2256 cm^{-1} which has not been observed by conventional IR and Raman spectra in these mixtures. The second derivatives of the IR spectra also show this new feature whose intensity increases with temperature, whereas the features at 2253 and 2259 cm^{-1} become weaker. Correspondingly, a new feature appears at about 3168 cm^{-1} for the combination band of the C≡N stretch and the C−C stretch, whereas the combination band of the free CH_3CN species is centered at 3164 cm^{-1}, and 3171 cm^{-1} for the hydrogen-bonded CH_3CN species. The new feature may be related to an intermediate microstructure between clusters of acetonitrile molecules and hydrogen-bonded acetonitrile molecules associated with clusters of water molecules. The results will provide useful structural and spectral information for the design of new 2D DOVE−FWM experiments and the molecular structure modeling of the mixtures.

Introduction

A newly developed coherent two-dimensional (2D) vibrational spectroscopy, doubly vibrationally enhanced four wave mixing (DOVE-FWM) spectroscopy has been recently demonstrated on a model system containing acetonitrile and water.[1] This method has high selectivity for component and structure determination by using two vibrational resonances.[1−6] Theoretical and experimental work has indicated that cross-peaks can only be observed if there is coupling between the vibrational modes.[1−8] According to general selection rules for the DOVE−FWM methods,[1−7] to observe the DOVE−Raman−FWM, an IR combination band of the two coupled modes is required. This combination band can be examined by measuring a conventional IR absorption spectrum. The presence of a combination band indicates a coupling between two fundamental modes.[1−7] Therefore, identification of combination bands in a model system becomes an interesting topic for the development of the DOVE−FWM methods.

Acetonitrile CH_3CN is a unique model system for the DOVE−FWM because it contains a highly environment-sensitive C≡N stretch mode (ν_2 at 2253 cm^{-1}) and a 3164-cm^{-1} combination band ($\nu_2 + \nu_4$) coming from the C≡N stretch and C−C stretch (ν_4 at 918 cm^{-1}). When acetonitrile is mixed with water, many experimental measurements and theoretical calculations indicate that the solution structure contains microheterogeneity.[9−15] X-ray diffraction shows that microheterogeneity occurs in the mixtures in the ranges of acetonitrile mole fractions $0.2 \leq x_{CH3}CN < 0.6$.[13] However, Raman spectroscopy by Reimers and Hall[11] indicates that no distinct point exists at which the onset of microheterogeneity starts. The observed onset may correspond simply to the limit of detectability.[11] It is generally agreed that in the mixtures, there are two types of CH_3CN molecules, free and hydrogen-bonded CH_3CN species.[9−15] This microstructural picture has guided us to develop the capabilities of the DOVE−FWM for component and structure determination by using CH_3CN-H_2O mixtures as a model for hydrogen-bonded systems in our preliminary work.[1−6] This general structure picture can be inferred from Figure 1 where two spectral regions for the ν_2 and $\nu_2 + \nu_4$ modes are presented. As shown in the region between 2220 and 2320 cm^{-1} for the ν_2 mode, in comparison with the 2253-cm^{-1} spectral feature of neat CH_3CN, the second derivative spectrum of a 50:50 mol % CH_3CN-H_2O solution shows an additional 2259-cm^{-1} feature at the higher energy side of the free CH_3CN species. This additional feature corresponds to the band of the hydrogen-bonded CH_3CN species.[9−13] Correspondingly, the $\nu_2 + \nu_4$ region also shows an additional 3171-cm^{-1} feature due to the hydrogen-bonded CH_3CN species. It is postulated that when one of the infrared lasers used in the DOVE−FWM is tuned into 2253 or 2259 cm^{-1}, only one DOVE−FWM peak at 3164 or 3171 cm^{-1}, corresponding to free or hydrogen-bonded CH_3CN species should be observed. Our preliminary experimental

* To whom correspondence should be addressed. E-mail: wxzhao@ualr.edu.

10.1021/jp020721f CCC: $22.00
Published on Web 06/26/2002

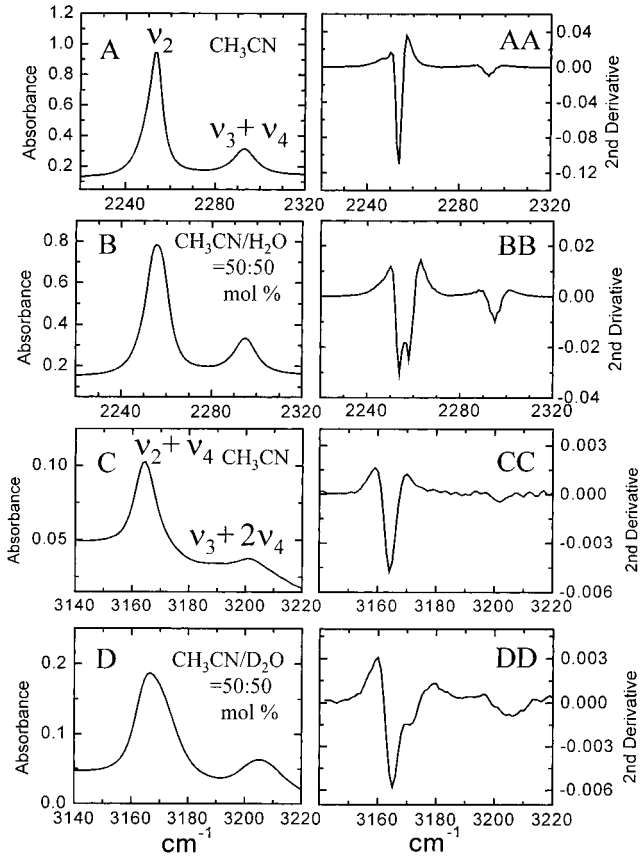

Figure 1. IR absorption spectra (A−D) and corresponding second derivative spectra (AA−DD) for neat acetonitrile, a 50:50 mol % CH_3CN-H_2O solution and a 50:50 mol % CH_3CN-D_2O solution at 25 °C.

result has indicated that only one of the expected DOVE−FWM peaks is observed when the laser is tuned into either 2253 or 2259 cm^{-1}.[1,16] The result indicates that the DOVE−FWM may be a snapshot of the local structure of the acetonitrile-water solution. Because the development of this unique DOVE−FWM relies on our knowledge of the model system's microstructure, it also becomes important to understand the microstructure of acetonitrile−water mixtures. In this work, we work on two areas of interest by using a highly sensitive 2D spectral method-2D IR correlation spectroscopy. First, we probe new microstructures in water-acetonitrile mixtures based on the highly environment-sensitive ν_2 mode. Second, we identify corresponding $\nu_2 + \nu_4$ combination bands of the probed microstructures. Temperature is used as a perturbation for constructing 2D IR correlation spectra.[17−25]

Experimental Section

Acetonitrile CH_3CN (purity 99.9%) and deuterated water D_2O (99.9%) were purchased from Aldrich. The water used for solution preparation was distilled. Three solutions used in this work were an acetonitrile (50 mol %)/H_2O (50 mol %) solution, an acetonitrile (50 mol %)/D_2O (50 mol %) solution, and an acetonitrile (38 mol %)/D_2O (62 mol %) solution.

A Nicolet Magna-FT-IR 550 spectrometer equipped with a DTGS−KBr detector, and a KBr beam splitter was used in the measurements at a resolution of 2 cm^{-1}. An FTIR temperature-controlled cell of WILMAD with CaF_2 windows and Teflon spacers was used for holding solutions. To optimize the signal-to-noise ratio, the path length was adjusted for different solutions and spectral ranges. The path length was 25 μm for the acetonitrile (50 mol %)/H_2O (50 mol %) solution, 50 μm for the acetonitrile (50 mol %)/D_2O (50 mol %) solution, and 100 μm for the acetonitrile (38 mol %)/D_2O (62 mol %) solution. The IR absorption spectra were collected as a function of temperature from 20 °C to 75 °C with 5 °C increments. A total of 64 scans were co-added for each spectrum. The measurement was repeated twice for each solution, and the reversibility of the change of the IR spectra upon temperature was also examined by cooling the heated solutions back to 25 °C, with 5 °C decrements.

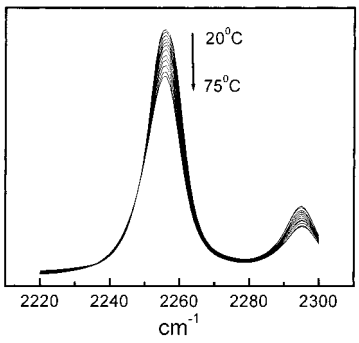

Figure 2. IR absorption spectra for the 50:50 mol % CH_3CN-H_2O solution measured under different temperatures.

2D IR correlation spectra were constructed using the generalized 2D correlation method developed by Noda under temperature perturbation.[17−19] The Hilbert transformation of the dynamic spectra was used for calculations.[19] An averaged spectrum was used as a reference for the 2D spectra constructed from original IR data, whereas no reference was used for the 2D spectra constructed from the second derivative data of the original IR spectra.[25] Microcal Origin, Mathcad and Matlab software packages were used to calculate and generate the 2D spectra. The negative cross-peaks in an asynchronous spectrum were shaded using the standard shading convention.[17,18] In a synchronous spectrum, a positive cross-peak at (ν_1, ν_2) indicates that the intensity changes at these two wavelengths are in the same direction. A positive asynchronous cross-peak at (ν_1, ν_2) indicates that the spectral change at ν_1 occurs earlier and at a lower temperature compared to ν_2. A negative asynchronous cross-peak indicates the opposite.[17−25]

Results and Discussion

It is observed that the intensities of all IR bands of CH_3CN in the 50:50 mol % CH_3CN-H_2O solution decrease with the increase of temperature. Figure 2 shows the temperature-dependent IR absorption spectra of the solution in the spectral region between 2220 and 2300 cm^{-1}. The ν_2 band is centered at about 2256 cm^{-1} and the $\nu_3 + \nu_4$ combination is centered at about 2295 cm^{-1}, where the ν_3 mode is assigned to the C−H bend at 1372 cm^{-1}.[1−3] No new features can be distinguished as the temperature increases. The 2D correlation spectra constructed from the data in Figure 2 are shown in Figure 3. In the 2D synchronous spectrum (Figure 3A), two autopeaks are observed at 2257 and 2295 cm^{-1}. For the autopeak at 2257 cm^{-1}, it has an elongated shape that is extended toward 2253 cm^{-1}, indicating that there are cross-peaks formed by the 2253 and 2257 cm^{-1} bands. A similar elongated positive cross-peak is observed at 2257/2295 cm^{-1}. The positive sign of the cross-peak indicates that both bands become weaker with the increase of the temperature.

The 2D asynchronous spectrum in Figure 3B has revealed new features. It is observed that around the autopeak at 2257 cm^{-1}, there are three peaks at 2253, 2256, and 2259 cm^{-1}. The 2253- and 2259-cm^{-1} bands have been assigned to the free and

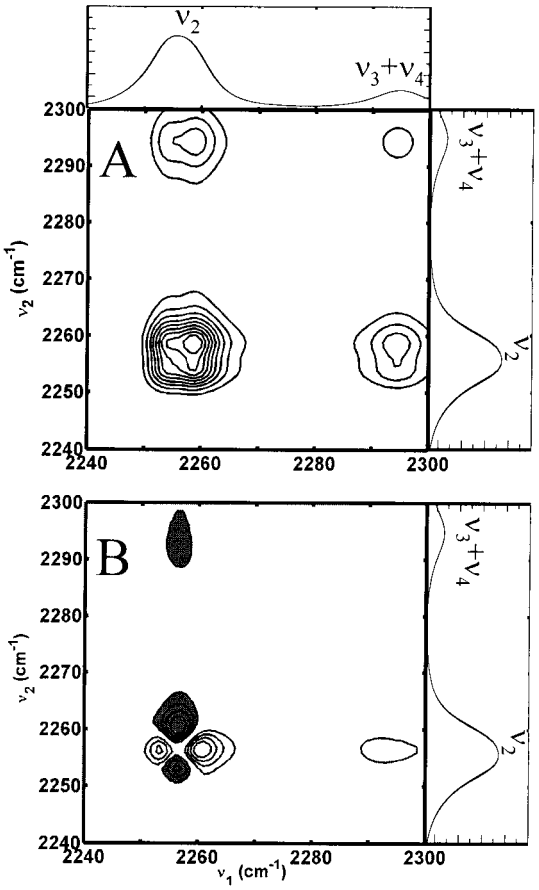

Figure 3. 2D synchronous (A) and asynchronous (B) correlation spectra for the 50:50 mol % CH_3CN-H_2O solution.

hydrogen-bonded CH_3CN species,[9−11] as shown in Figure 1BB. The spectral feature at 2256 cm^{-1} has not been observed before. This band forms three positive cross-peaks, 2253/2256, 2259/2256, and 2295/2256 cm^{-1}, with the 2253-, 2259-, and 2295-cm^{-1} bands, respectively. The presence of the new 2256-cm^{-1} band may indicate that a new microstructure develops when the solution temperature increases. The evolution of this new structure can be examined from the cross-peaks around 2253 cm^{-1}. The two positive cross-peaks 2253/2256 and 2259/2256 cm^{-1} suggest that with the increase of temperature, the 2253- and 2259-cm^{-1} bands change prior to the 2256-cm^{-1} band. The lack of cross-peak 2253/2259 cm^{-1} in the 2D asynchronous correlation spectrum indicates that these two features have similar temperature dependence, i.e., their intensities all decrease with the temperature. Thus, we can infer that with the increase of the temperature, the microstructure related to the 2256-cm^{-1} feature gains with the cost of the free and hydrogen-bonded CH_3CN species located at 2253 and 2259 cm^{-1}.

To confirm this observation, we have also calculated the second derivative data based on the temperature-dependent IR spectra in Figure 2. From the second derivative spectra shown in Figure 4, we were surprised to find a new feature at 2256 cm^{-1} which becomes quite clear at about 40 °C. This feature evolves when the temperature increases. Meanwhile, the bands at 2253 and 2259 cm^{-1} become weaker.

The agreement between the 2D asynchronous correlation spectrum and the second derivative spectra leads us to conclude that there is a new CH_3CN species existing in the water−acetonitrile mixture instead of only the free and the hydrogen-bonded species previously suggested. As shown in Figure 4, this new feature can even be observed below 40 °C. It may

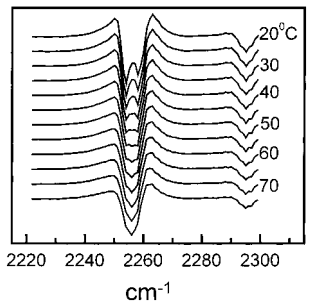

Figure 4. Second derivative spectra of the IR absorption spectra of the 50:50 mol % CH_3CN-H_2O solution in Figure 2 under different temperatures. The spectra are plotted on the same scale but shifted with equal division for clarity.

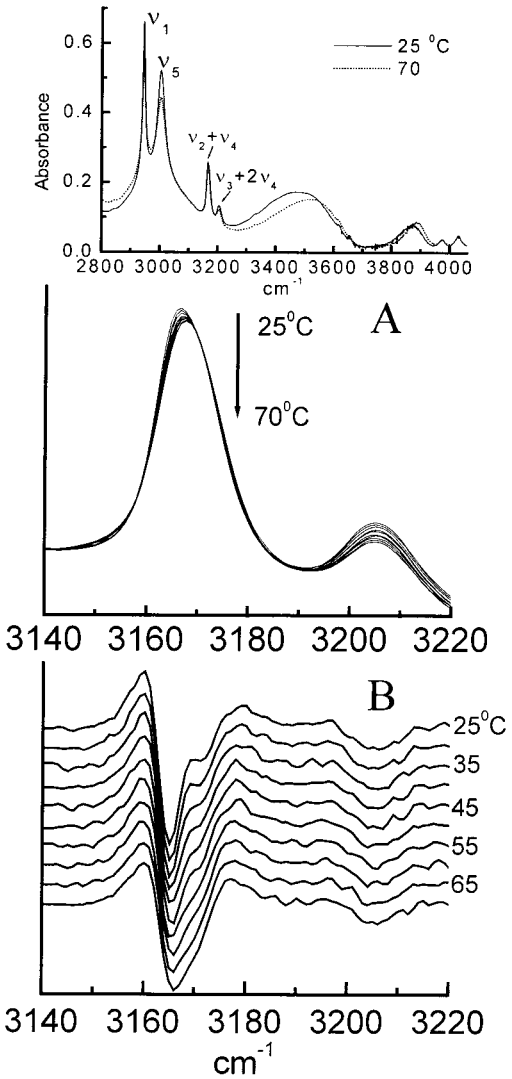

Figure 5. IR absorption spectra (A) and their second derivative spectra (B) for a 50:50 mol % CH_3CN-D_2O solution under different temperatures. The second derivative spectra are plotted on the same scale but shifted with equal division for clarity. The inset shows an extended region between 2800 and 4060 cm^{-1} where the ν_1 and ν_5 are the C−H stretch modes.

also exist at room temperature, but is buried in the spectral overlap of the free and hydorgen-bonded species. It evolves at higher temperatures where it is easier to observe.

Because there are corresponding combination bands in the $\nu_2 + \nu_4$ spectral region for free and hydrogen-bonded CH_3CN species, there is a question whether this new species also has a corresponding $\nu_2 + \nu_4$ combination band so that new DOVE−

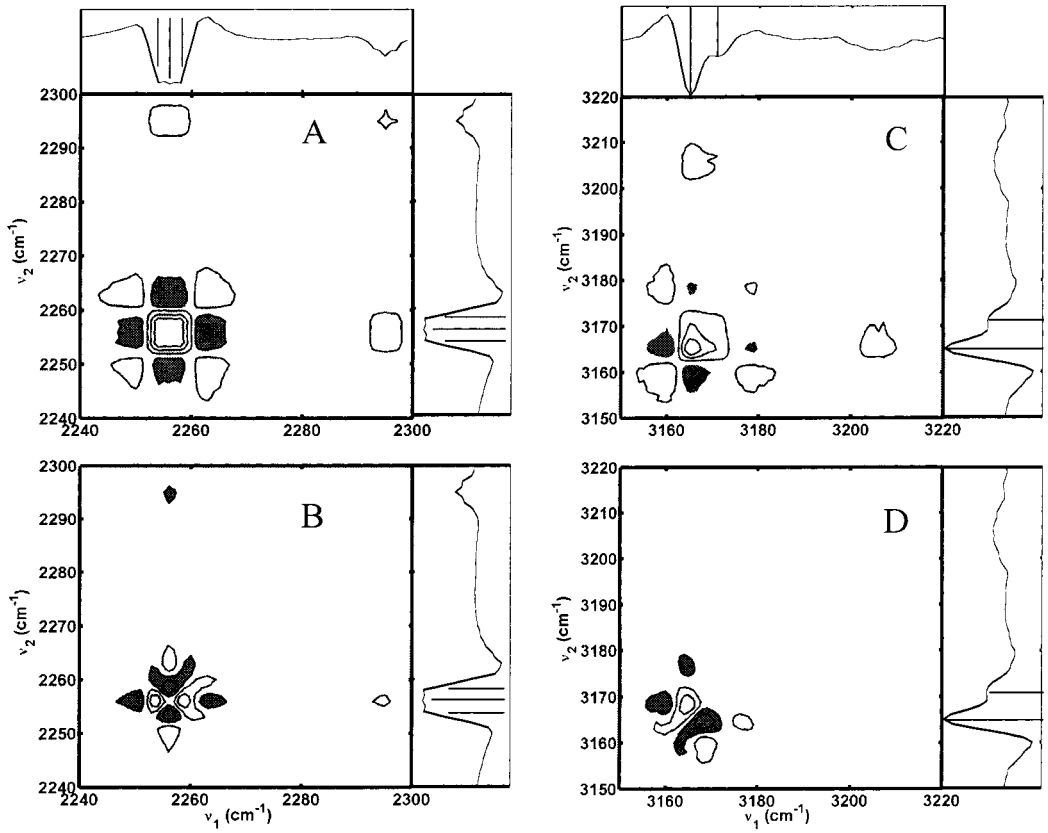

Figure 6. 2D synchronous (A) and asynchronous (B) correlation spectra in the ν_2 spectral region and 2D synchronous (C) and asynchronous (D) correlation spectra in the $\nu_2 + \nu_4$ spectral region constructed from the second derivative spectra in Figure 4 for the 50:50 mol % CH_3CN-H_2O solution and in Figure 5B for the 50:50 mol % CH_3CN-D_2O solution.

FWM experiments could be conducted for this new species. With this question in mind, we have examined the spectral region of the $\nu_2 + \nu_4$ combination band for probing the spectral feature of the new species.

Because the strong absorption band of O−H stretch of H_2O obscures the observation of the $\nu_2 + \nu_4$ combination band at about 3164 cm^{-1} for water−acetonitrile mixtures,[1] deuterated water D_2O is used to replace H_2O. The temperature-dependent IR absorption spectra of a 50:50 mol % CH_3CN-D_2O solution are shown in Figure 5A in the range of 3140−3220 cm^{-1}. The corresponding second derivative spectra are shown in Figure 5B. From the second derivative spectra, we can see that the feature at about 3171 cm^{-1} becomes stronger with the increase of temperature. If there is a feature related to the new species, then its position should locate at about 3168 cm^{-1}, in the middle of the 3164- and 3171-cm^{-1} bands. From Figure 5, it is hard to tell whether there is such a feature because of spectral overlapping.

The 2D spectra may provide additional information. For constructing 2D spectra, directly using the data of the IR spectra in the range of 3140−3220 cm^{-1} is unreliable because of the inconsistent spectral background for the $\nu_2 + \nu_4$ combination which varies with temperature. The inconsistent spectral background mainly comes from the contribution of the broad 3500-cm^{-1} O−H stretch band which shifts toward the blue when the temperature increases as shown in the inset of Figure 5. The O−H group comes from the contaminated H_2O, which is introduced after the solution is exposed to the moist air during the solution preparation and the step of transferring the solution into the IR cell. The fluctuation in the spectral background may distort the 2D spectra and should be avoided.[22] Because the background is relatively broad and can be eliminated in the second derivative spectra, we decide to use the second derivative data in Figure 5B for constructing 2D spectra by following the suggestion of Czarnecki.[22]

Before we construct the 2D spectra in the spectral range of 3140−3220 cm^{-1} by using the second derivative data in Figure 5B, we have also used the second derivative data in the spectral range of 2240−2300 cm $^{-1}$ in Figure 4 to construct the 2D spectra in order to examine the reliability of using the second derivative data for 2D spectra. In the 2D synchronous spectrum (Figure 6A), only meaningful autopeaks are found at around 2254 and 2295 cm^{-1}. They form two positive cross-peaks (2254 vs 2295 cm^{-1}). The rest around the 2254-cm^{-1} peak is the satellite peaks which are not related to new spectral features. Instead, they are due to the side lobes shown in the second derivative spectra.[22]

In the asynchronous spectrum (Figure 6B), we can see two positive cross-peaks 2253/2256 and 2259/2256 cm^{-1} and two negative cross-peaks at 2256/2253 and 2256/2259 cm^{-1} in the ν_2 spectral region. The satellite peaks around these cross-peaks are also due to the side lobes shown in the second derivative spectra. In addition, there is a pair of cross-peaks at 2295/2256 and 2256/2295 cm^{-1}. In comparison with the 2D spectra in Figure 3, the same information can be extracted from the second derivative-based 2D correlation spectra. So the second derivative-based 2D spectra may also provide reliable information regarding the spectral features in the range of 3140−3220 cm^{-1}.

The 2D spectra constructed from the second derivative spectra in Figure 5B are shown in Figure 6 C and D. In the 2D synchronous spectrum, an autopeak centered at around 3164 cm^{-1} is observed with elongated cross-peaks at about 3165−3172 cm^{-1}. The satellite peaks around this autopeak come from the side lobes in the second derivative spectra, not indicating

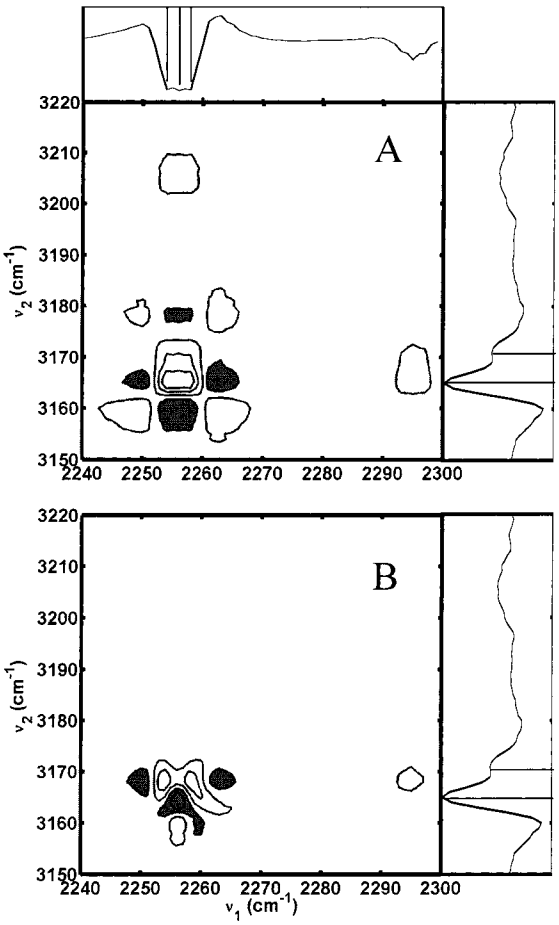

Figure 7. 2D synchronous (A) and asynchronous (B) correlation heterospectra constructed from the second derivative data in Figure 4 and Figure 5B.

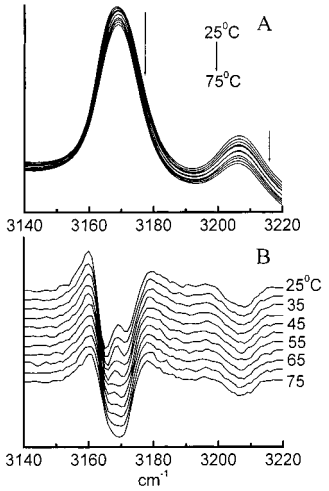

Figure 8. IR absorption spectra (A) and their second derivative spectra (B) for a 38:62 mol % CH_3CN-D_2O solution under different temperatures. The second derivative spectra are plotted on the same scale but shifted with equal division for clarity.

new features. Positive cross-peaks (3164 vs 3205 cm^{-1}) are also observed, indicating the intensity of both 3164 and 3205 cm^{-1} peaks changes in the same direction, i.e., decreases with temperatures.

In the 2D asynchronous spectrum in Figure 6D, only two cross-peaks (3164 vs 3168 cm^{-1}) are observed, with four side lobes-related satellite peaks. The 3164-cm^{-1} band is assigned to the free CH_3CN species, whereas the 3168-cm^{-1} peak is a new feature revealed in the asynchronous spectrum because it is located at expected position for the new species. It may be the spectral feature that we are looking for. The sign of the cross-peaks indicates that the 3164-cm^{-1} band changes before the 3168-cm^{-1} band, which is consistent with the spectral change sequence in the ν_2 spectral region where the intensity of the free CH_3CN species changes before that of the new species.

To further reveal the phase relationship for these CH_3CN species between the ν_2 spectral region and the $\nu_2 + \nu_4$ spectral region, 2D correlation heterospectra are constructed as shown in Figure 7. The out-of-phase correlation can be clearly seen from the asynchronous spectrum. Three cross-peaks are observed at 2253/3168 (positive), 2256/3164 (negative), and 2259/3168 cm^{-1} (positive), with three satellite peaks formed from the side lobes. There is also a cross-peak at 2295/3168 cm^{-1}. These cross-peaks confirm that the 3168-cm^{-1} feature is not in-phase with the 2253- and 2259-cm^{-1} features. They may come from different CH_3CN species. In addition, For the 2253- and 3164-cm^{-1} bands, they belong to the free CH_3CN species, so no cross-peak between them is observed. No cross-peak at 2256/3168 cm^{-1} also suggests that the 3168-cm^{-1} band has a similar temperature dependence to the 2256-cm^{-1} band which comes from the new species. Therefore, 3168-cm^{-1} band is the feature that we are looking for in the $\nu_2 + \nu_4$ spectral region for the new species.

Because in the ν_2 spectral region, we observe the cross-peaks for the 2259-cm^{-1} band of hydrogen-bonded species, we should also have observed the cross-peaks for the 3171-cm^{-1} band of hydrogen-bonded species in the $\nu_2 + \nu_4$ spectral region. As we further examine the cross-peaks in the $\nu_2 + \nu_4$ combination band-related 2D asynchronous spectra (Figure 6D and Figure 7B), those cross-peaks are not presented, which should have given cross-peaks at 3168/3171 and 3171/3168 cm^{-1} in Figure 6D, and 2256/3171 cm^{-1} in Figure 7B for hydrogen-bonded species-related modes. The unresolvable of these cross-peaks may be due to the two possible spectral causes related to the 3171-cm^{-1} feature: (i) the relatively low intensity as shown in Figure 1DD as compared with the intensity of the 2259-cm^{-1} band in Figure 1BB, and (ii) the relatively broad bandwidth of the $\nu_2 + \nu_4$ combination band as shown in Figure 1CC as compared with the bandwidth of the ν_2 band in Figure 1AA. These two causes may make these cross-peaks not easy to observe.

To confirm whether these two causes play a role in the result, we have prepared a 38:62 mol % CH_3CN-D_2O solution. The solution has a similar second derivative line shape (Figure 8B) of the $\nu_2 + \nu_4$ combination band at 25 °C to that of the ν_2 band of the 50:50 mol % CH_3CN-H_2O solution (Figure 1BB). From the temperature-dependent IR spectra of the 38:62 mol % CH_3CN-D_2O solution (Figure 8A), we can see that the intensity of the bands decreases with temperature. In the second derivative spectra (Figure 8B), two bands with almost equal intensity are identified at 3164 and 3173 cm^{-1} at 25 °C. The 3164 cm^{-1} band assigned to free CH_3CN species seems not to change its position with the concentration of water. The 3173-cm^{-1} band is assigned to hydrogen-bonded CH_3CN species whose position shifts to blue when the water content increases. At higher temperatures, both bands become weaker and a new band emerges at about 3169 cm^{-1}. This new band can be easier to see from a 2D asynchronous spectrum in Figure 9.

In Figure 9, we can observe two positive cross-peaks 3164/3169 and 3173/3169 cm^{-1} in the $\nu_2 + \nu_4$ spectral region. The 3173-cm^{-1} band of hydrogen-bonded CH_3CN species appears, together with the 3169-cm^{-1} band of the new species. So this

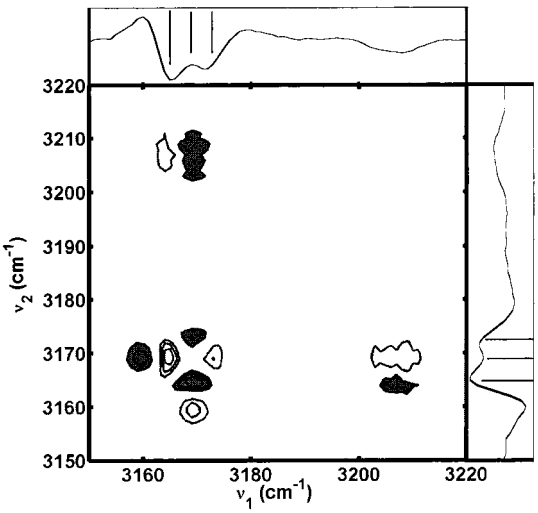

Figure 9. 2D asynchronous spectrum in the $\nu_2 + \nu_4$ spectral region constructed from the second derivative spectra in Figure 8B for the 38:62 mol % CH_3CN-D_2O solution.

result further confirms that the new species has a corresponding $\nu_2 + \nu_4$ combination band as observed in Figure 6D and Figure 7B. It also verifies the two spectral causes which are responsible for the unresolvable of the 3171-cm^{-1} band of hydrogen-bonded species in the 2D spectra of the 50:50 mol % CH_3CN-D_2O solution.

The detailed microstructure of the observed new CH_3CN species is not quite clear. Because this new species gains with the consumption of free CH_3CN species and hydrogen-bonded CH_3CN species when the temperature increases, it could be an intermediate hydrogen-bonded CH_3CN species between free CH_3CN species and hydrogen-bonded CH_3CN species associated with water clusters. This intermediate species should have less water clusters interacted, in comparison with the hydrogen-bonded CH_3CN species. For the water clusters associated with the hydrogen-bonded species, Bertie and Lan[9] and Jamroz et al.[10] have suggested that they could be linear chains of water molecules rather than spherical clusters. Bertie and Lan[9] and Reimers and Hall[11] have used a 1:1 molar ratio of CH_3CN to H_2O in the bound region to interpret their IR[9] and Raman[11] spectra of the mixtures. To explain the concentration-dependent blue-shift of the bound ν_2 band, Reimers and Hall[11] have postulated that CH_3CN may form up to two hydrogen bonds to water with a corresponding increase in water's donation to CH_3CN. If the 2259-cm^{-1} band is assigned to the hydrogen-bonded CH_3CN species with a 1:2 molar ratio of CH_3CN to H_2O, then the 2256-cm^{-1} band could be due to the hydrogen-bonded CH_3CN species with a 1:1 molar ratio of CH_3CN to H_2O. Further molecular structure modeling may provide useful information about the microstructure of this new species observed here.

More importantly, the identification of the new species and its corresponding fundamental and combination bands in this work allows us to design new 2D DOVE−FWM experiments for the snapshot of the local structure of the observed new species in acetonitrile−water mixtures by probing the cross-peak at about 2256/3168 cm^{-1}. The presence of the cross-peak in the DOVE−Raman−FWM spectra will confirm the results observed in this work. The exact band positions can also be determined from the cross-peaks in the DOVE−FWM spectra, which could address the concern regarding the interpretation of the band positions in an asynchronous spectrum.[26] The DOVE−FWM spectra will provide complementary results regarding the band positions to other methods including the Fourier self-deconvolution and the second derivatives.[27−30] Moreover, the knowledge gained from this work will help us to theoretically model the DOVE−FWM spectra by using the improved microstructure picture of the mixtures.

Conclusions

Understanding the microstructure of the model system acetonitrile−water mixtures is important for the development of the DOVE−FWM spectroscopic methods for the structure analysis and component determination of hydrogen-bonded systems. By using the sensitive 2D IR correlation spectroscopy, we have revealed a new CH_3CN species with a C≡N stretch band position at 2256 cm^{-1} and a $\nu_2 + \nu_4$ combination band position at about 3168 cm^{-1}. This observation suggests that the general microstructure picture of the mixtures with two types of CH_3CN species should be improved by involving more than two species. It will provide useful information for the design of new 2D DOVE−FWM experiments and theoretical modeling of the 2D DOVE−FWM experimental data for the mixtures in order to understand the power of this unique coherent 2D vibrational spectroscopy.

Acknowledgment. Wei Zhao acknowledges the financial support from the Cottrell College Science Award of Research Corporation. He also thanks Prof. John C. Wright for his proofreading the manuscript during his short visit at the University of Arkansas-Little Rock as a distinguished invited speaker.

References and Notes

(1) Zhao, W.; Wright, J. C. *J. Am. Chem. Soc.* **1999**, *121*, 10 994.
(2) Zhao, W.; Wright, J. C. *Phys. Rev. Lett.* **1999**, *83*, 1950.
(3) Zhao, W.; Wright, J. C. *Phys. Rev. Lett.* **2000**, *84*, 1411.
(4) Besemann, D. M.; Condon, N. J.; Murdoch, K. M.; Zhao, W.; Meyer, K. A.; Wright, J. C. *Chem. Phys.* **2001**, *266*, 177.
(5) Zhao, W.; Murdoch, K. M.; Besemann, D. M.; Condon, N. J.; Meyer, K. A.; Wright, J. C. *Appl. Spectrosc.* **2000**, *54*, 1000.
(6) Murdoch, K. M.; Condon, N. J.; Zhao, W.; Besemann, D. M.; Meyer, K. A.; Wright, J. C. *Chem. Phys. Lett.* **2001**, *335*, 349.
(7) Wright, J. C.; Chen, P. C.; Hamilton, J. P.; Zilian, A.; Labuda, M. J. *Appl. Spectros.* **1997**, *51*, 949.
(8) Tanimura, Y.; Mukamel, S. *J. Chem. Phys.* **1993**, *99*, 9496.
(9) Bertie, J. E.; Lan, Z. *J. Phys. Chem. B* **1997**, *101*, 4111.
(10) Jamroz, D.; Stangret, J.; Lindgren, J. *J. Am. Chem. Soc.* **1993**, *115*, 6165.
(11) Reimers, J. R.; Hall, L. E. *J. Am. Chem. Soc.* **1999**, *121*, 3730.
(12) Easteal, A. J. *Aust. J. Chem.* **1979**, *32*, 1379.
(13) Takamuku, T.; Tabata, M.; Yamaguchi, A.; Nishimoto, J.; Kumamoto, M.; Wakita, H.; Yamaguchi, T. *J. Phys. Chem. B* **1998**, *102*, 8880.
(14) Nishikawa, K.; Kasahara, Y.; Ichioka, T. *J. Phys. Chem. B* **2002**, *106*, 693.
(15) Baldelli, S.; Mailhot, G.; Ross, P. N.; Somorjai, G. A. *J. Am. Chem. Soc.* **2001**, *123*, 7697.
(16) Zhao, W.; Wright, J. C., unpublished results.
(17) Noda, I. *Appl. Spectrosc.* **1993**, 47, 1329.
(18) Ozaki, Y.; Liu, Y.; Noda, I. *Appl. Spectrosc.* **1997**, *51*, 526.
(19) Noda, I. *Appl. Spectrosc.* **2000**, *54*, 994.
(20) Ren, Y.; Shimoyama, M.; Ninomiya, T.; Matsukawa, K.; Inoue, H.; Noda, I.; Ozaki, Y. *Appl. Spectrosc.* **1999**, *53*, 919.
(21) Ren, Y.; Murakami, T.; Nishioka, T.; Nakashima, K.; Noda, I.; Ozaki, Y. *J. Phys. Chem. B* **2000**, *104*, 679.
(22) Czarnecki, M. A. *Appl. Spectrosc.* **1998**, *52*, 1583.
(23) Pancoska, P.; Kubelka, J.; Keiderling, T. A.; *Appl. Spectrosc.* **1999**, *53*, 655.
(24) Sefara, N. L.; Magtoto, N. P.; Richardson, H. H. *Appl. Spectrosc.* **1997**, *51*, 536.
(25) Schultz, C. P.; Barzu, O.; Mantsch, H. H. *Appl. Spectrosc.* **2000**, *54*, 931.
(26) Comments of one reviewer.
(27) Czarnecki, M. A. *Appl. Spectrosc.* **2000**, *54*, 1767.
(28) Evans, J. N. S. *Biomolecular NMR Spectroscopy*, Oxford University Press: New York, 1995.
(29) Dong, A.; Huang, P.; Caughey, W. S. *Biochemistry* **1990**, *29*, 3303.
(30) Lee, D. C.; Herzyk, E.; Chapman, D. *Biochemistry* **1987**, *26*, 5775.